Feasibility of sub-dermal soft tissue deformation assessment using B-mode ultrasound for pressure ulcer prevention

J. Doridam[a,c,*], A. Macron[a,b], C. Vergari[a], A. Verney[b], P.-Y. Rohan[a], H. Pillet[a]

[a] *Arts et Métiers ParisTech, LBM/Institut de Biomécanique Humaine Georges Charpak, 151 bd de l'Hôpital, 75013, Paris, France*
[b] *CEA, LIST, Interactive Robotics Laboratory, F-91191, Gif-sur-Yvette, France*
[c] *Department of Anatomy, University Paris XIII, UFR Santé Médecine Biologie Humaine, Bobigny, France*

Keywords:
pressure ulcer
Ultrasound
Subdermal soft tissue
Strains

A B S T R A C T

Pressure Ulcer (PU) prevention remains a main public health issue. The physio-pathology of this injury is not fully understood, and a satisfactory therapy is currently not available. Recently, several works suggested that mechanical strains are responsible of deformation-induced damage involved in the initiation of Deep Tissue Injury (DTI). A better assessment of the internal behavior could allow to enhance the modeling of the transmission of loads into the different structures composing the buttock. A few studies focused on the experimental in vivo buttock deformation quantification using Magnetic Resonance Imaging (MRI), but its use has important drawbacks. In clinical practice, ultrasound imaging is an accessible, low cost, and real-time technic to study the soft tissue. The objective of the present work was to show the feasibility of using B-mode ultrasound imaging for the quantification of localised soft-tissue strains of buttock tissues during sitting. An original protocol was designed, and the intra-operator reliability of the method was assessed. Digital Image Correlation was used to compute the displacement field of the soft tissue of the buttock during a full realistic loading while sitting. Reference data of the strains in the frontal and sagittal planes under the ischium were reported for a population of 7 healthy subjects. The average of shear strains over the region of interest in the fat layer reached levels up to 117% higher than the damage thresholds previously quantified for the muscular tissue in rats. In addition, the observation of the muscles displacements seems to confirm previous results which already reported the absence of muscular tissue under the ischium in the seated position, questioning the assumption commonly made in Finite Element modeling that deep tissue injury initiates in the muscle underlying the bone.

1. Introduction

Pressure Ulcer (PU) prevention remains a main public health issue, by its human and financial cost with extended hospitalization, decreased quality of life and loss of autonomy [1–3]. Two types of PU can be identified: one superficial developing from the skin and another developing from the deep soft tissue which, in an advanced stage, progressively extends to the skin [4–6,7]. These deep lesions, called Deep Tissue Injuries (DTI), are more severe because of the late time of diagnosis and sometimes may require surgical intervention. Spinal Cord Injury (SCI) patients are especially concerned. The development of PU due to reduced mobility and neurosensorial loss remains frequent in these patients, with a prevalence of 33% in the first year, and an incidence of 80% during the whole life [8,9]. Due to prolonged sitting position and wheelchair use, the pelvic area is the most frequent location of PU in these patients, with about 64% in the ischiatic area [7,10]. Recommendations for PU prevention have been established in clinical practice based on pressure relief strategies with patient mobilization and specific pressure-relieving cushion [1,11]. Despite these, PU prevalence still remains high [2,3]. More efficient prevention necessitates a better understanding of the underlying physiopathological mechanism.

PU are provoked by compression of the soft tissues between an external surface and a bony prominence. Compression-induced ischemia is known to be a major factor of PU onset [12,13]. More recently, several experimental works suggested that damage involved in the initiation of DTI are tightly related to localized soft tissue strains [13–15]. Indeed, Stekelenburg et al. showed for the left tibialis of rats that the combination of deformation with ischemia decreased the time for irreversible damage compared to ischemia alone [12]. Moreover, the damages were evident when the shear strains (Cauchy Green formulation) endured by the muscle were above 75% [4]. Gefen et al.

further showed that at 77% of deformation, instantaneous cell death could be observed in bio-artificial muscles [16].

Few works focused on in vivo buttock deformation quantification by MRI imaging. Sonenblum et al. used 3D seated Magnetic Resonance Imaging (MRI) to describe the anatomy and deformation of the buttocks for 4 able-bodied and 3 SCI subjects during sitting in loaded and unloaded conditions [17]. They highlighted important variation between soft tissue behaviors under the ischial tuberosity (IT) in the different subjects. The authors showed that, in the loaded configuration, 5 subjects out of 7 only had fat tissue beneath the IT, the Gluteus Maximus (GM) being positioned more laterally and posteriorly to the IT. In the loaded configuration, only one of the subject had a GM muscle thickness of 8 mm beneath the IT. The authors highlighted that this observation was inconsistent with the assumptions dominating the literature, focusing on localized muscle strains either in experimental studies on rats or in numerical simulations in humans. Yet, the reported results suggest that the muscle, particularly the GM is often not directly loaded by the bone. Likewise, Call et al. observed, using MRI, that, in a population of 10 spinal cord injury subjects and one able-bodied person, no muscle were present beneath the IT for 40% of the SCI subjects during sitting [18]. They concluded that this lack of muscle in the SCI population compared to healthy people decreased the overall soft tissue thickness, increasing the risk of tissue damage over bony prominences. None of these studies quantified internal deformation. On the contrary, Solis and al. assessed internal deformation in vivo in 5 healthy and 2 SCI pigs using tagged MRI [19]. They demonstrated that relatively low levels of external loads are capable of generating high magnitudes of strain in the loaded muscles, particularly in atrophied muscles. They also observed that compressive strains were higher in the SCI pigs than in the healthy sample. However, this technic is based on the assumption of small deformations, which is not the case in biological soft tissues in normal loading. As the authors reported, when the deformation in the tissue becomes too large, the tag lines become indiscernible and strain vectors can no more be measured. It is important to stress that Solis et al. are the only research team to have quantified localized soft tissue strains in the buttock region in vivo but only on an animal model. In short, if MRI is a potential tool for the quantitative evaluation of subdermal soft tissue strains, it has important drawbacks including long acquisition time, examination cost and confined environment.

Because of the experimental difficulties associated with the estimation of the localised strains deformation in soft tissue during sitting, some research teams have developed finite element models of the buttock region [20–22]. FE is a powerful tool to improve the understanding of pressure ulcer formation near the ischium because it allows to study the impact of relative influence of individual parameters, soft tissue mechanical properties and testing in many conditions. Even if partial validation based on external envelope shape or external pressure measurement [23] were reported, no direct validation of localized soft tissue strains has been performed. Yet, these localized soft tissue strains are paramount because they are currently the only mechanical parameter known to be responsible of the onset of DTI. Moreover, the assumptions on which these models rely often simplified both the anatomy and the relative interaction between the internal components such as the sliding between muscles. A better assessment of the internal behavior could allow to enhance the modeling of the transmission of loads into the different structures composing the buttock.

In clinical practice, ultrasound imaging is an accessible, low cost, and real-time technic to study the soft tissue [24]. Moreover, ultrasound imaging has been shown to be promising for the quantification of localized soft tissue strains using Digital Image Correlation (DIC) techniques [25]. It has been used, for example, *in vitro*, in tissue-mimicking phantom [26] and, in vivo, in the human Achilles tendon [27] and in the quadriceps muscle [28]. The extension to buttock tissue should contribute to a better understanding of the behavior of subdermal tissues in this region during loading.

The objective of the present work was to determine the feasibility of B-mode ultrasound imaging for the quantification of localized soft tissue strains of buttock soft tissues during sitting. The intra-operator reliability of the method will be assessed and reference data on a population of 7 healthy subjects will be given.

2. Materials and method

2.1. Subjects and preparation

Seven subjects participated to the experiment, 1 woman and 6 men (Age: 28 ± 4 yrs, Weight: 75 ± 10 kg, BMI: 23.2 ± 2.0 kg/m^2). After approval by the ethics committee (Comité de protection des Personnes CPP NX06036) and written informed consent, the subjects were equipped with 4 reflective markers on the anterior and posterior iliac spines of the pelvis and one on the spinal process of the 4 t h lumbar vertebra.

2.2. Ultrasound acquisitions

An ultrasound acquisition of the subdermal tissue in the region beneath the ischial tuberosity was performed using a commercial device (Aixplorer, SuperSonic Imagine, France) with a linear ultrasound probe of 8 MHz central frequency (SuperLinear SL 15-4). Simultaneously, the 3D position of the markers were recorded using a optoelectronic system (Vicon, Vicon Motion Systems Ltd., Oxford, UK).

A custom-made stool was used for the experiment. A cross-shaped notch was made in the seat to fix the ultrasound probe in two orthogonal positions (Fig. 1). In order to ensure a good fit between the cross-shaped notch and the probe, the space was filled with a custom made 3D printed part. Special care was paid to the design so as to ensure a flat surface in the vicinity of the probe. The stool was equipped with 3 optoelectronic markers.

The subject was asked to sit on the stool in front of the on-screen display of the ultrasound device. After covering of the probe with echography gel, two video clips were acquired: the first one with the probe in the frontal plane and the second one in the sagittal plane (Fig. 1). For each acquisition, the subject was instructed to align his left ischium above the probe, to adjust his position to see the bone at the center of the screen and then to slowly unload his weight with his arms while visually keeping the ischium as aligned as possible with the probe.

2.3. Data analysis

2.3.1. Image processing and strain calculation

Digital Image Correlation (DIC) was used to quantify localized soft tissue strains in the muscle and fat layers using a custom software written in Matlab (2014b) (MathWorks, Inc, Natick MA) [34]. First, a rectangular Region Of Interest (ROI) was defined manually in the first image and discretized into a grid of 21 points (3 × 7). These points were then automatically tracked in each successive frame using a normalized 2-D cross-correlation algorithm. The position of the points could be manually corrected if necessary. From the positions of the points, a displacement field was calculated at each frame as described below.

The deformation gradient tensor F and the Green-Lagrange strain tensor E were computed from the displacement field for each point of the grid as following:

$$\boldsymbol{F_{ij}} = \frac{\boldsymbol{dx_i}}{\boldsymbol{dX_j}} = \begin{bmatrix} \frac{dx_1}{dX_1} & \frac{dx_1}{dX_2} \\ \frac{dx_2}{dX_1} & \frac{dx_2}{dX_2} \end{bmatrix} \tag{1}$$

$$\boldsymbol{E} = \frac{1}{2}(\boldsymbol{F^T F} - I) \tag{2}$$

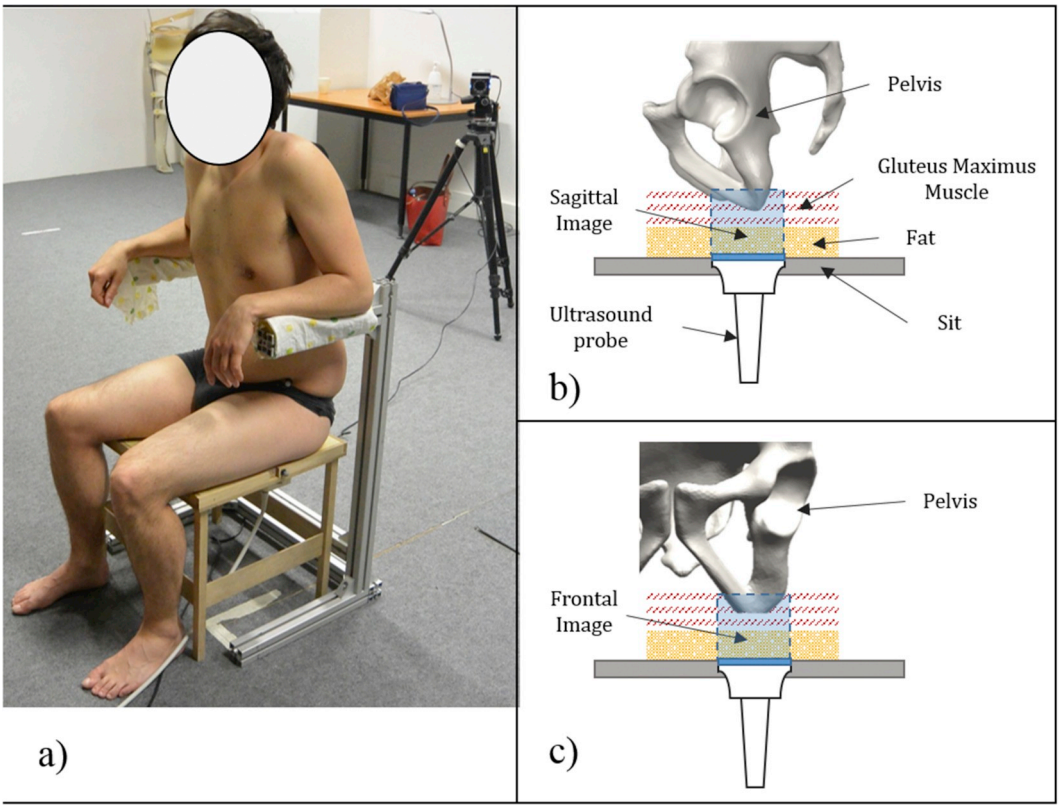

Fig. 1. a) Diagram showing the position of the subject during the ultrasound acquisition b) and c) sagittal and frontal positions of the ultrasound probe with respect to the pelvis.

$$E_{Shear} = \frac{1}{2}|E_I - E_{II}| \quad (3)$$

Here, x_i is the position of the grid points in the ith image and X in the initial image. The Green Lagrange tensor E were diagonalized to quantify the first and the second principal strains: respectively E_I and E_{II}. These were used to estimate the shear strains E_{Shear} using equation (3).

The first and the second principal strains in the ultrasound frontal and sagittal planes are illustrated in Fig. 2.

2.3.2. Reproducibility

Intra-operator reproducibility of the shear strain was also assessed. For each subject and for each acquisitions (in respectively the frontal and sagittal planes), one operator performed 4 times the whole procedure. Each time, the initial grid was automatically positioned in the fat layer. For each point *i* of the grid, the variance (S_i^2) among the trials was calculated as follows:

$$x_{ik} = E_{ik} - \overline{E_i} \quad (4)$$

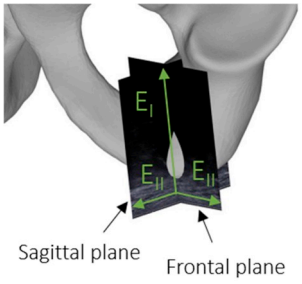

Fig. 2. Illustration of the principal directions in the frontal and sagittal planes.

$$S_i^2 = \frac{\sum_{k=1}^{N}(x_{ik} - \overline{x_i})^2}{N_i} \quad (5)$$

where $\mathbf{E_{ik}}$ is the shear strain of the ith point for the kth trial, N the number of trials and $\overline{E_i}$ the mean shear strain of the ith point among the trials.

Si was computed as an estimator of the error of reproducibility.

2.3.3. Calculation of the horizontal rotation of the pelvis

In order to quantify the change in orientation of the pelvis between the two ultrasound acquisitions, a local pelvis frame (R_p) was constructed from the anterior and posterior iliac spines markers. For each acquisition, the position of this frame was expressed in a local frame attached to the stool (R_c) and the orientation matrix of the relative position of R_p between both acquisitions was calculated. Then, the angle around the vertical axis of the pelvis between both configurations was computed for each subject by decomposition of the rotation matrix.

3. Results

3.1. Calculation of the horizontal rotation of the pelvis

For all the subjects, the horizontal rotation of the pelvis between the frontal and sagittal acquisitions was below 8°.

3.2. Distribution of the internal deformation of the soft tissues

Fig. 4 below shows the deformation of the subdermal soft tissues during sitting for one typical subject.

Strain measurement was possible for all subjects in the fat layer. Due to the limited acquisition field inherent to the use of ultrasound probes, the monitoring of the muscle tissue during the whole acquisition was not always possible.

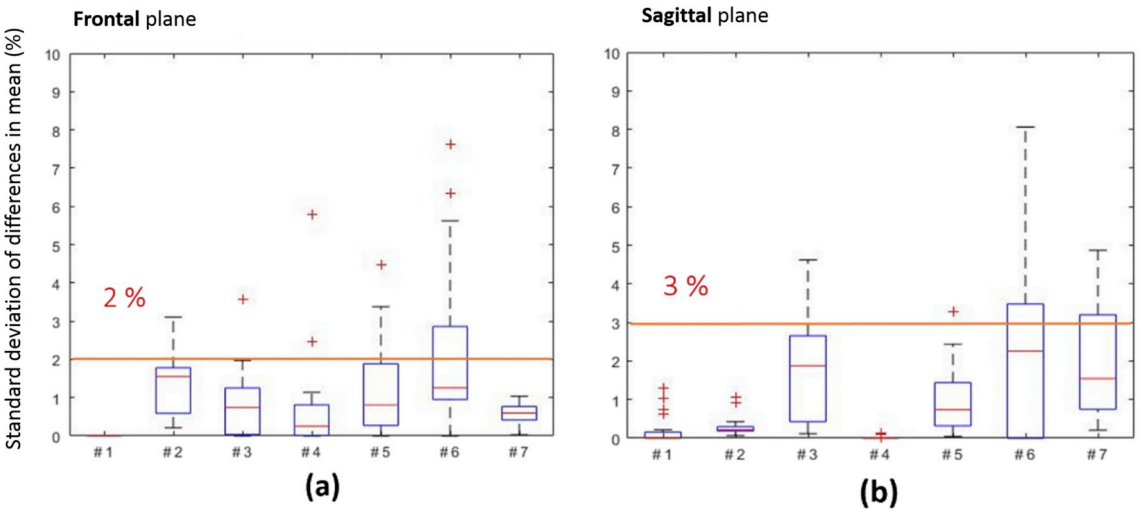

Fig. 3. a) box-plot of the error of reproducibility S_i of the shear strain in the (a) frontal plane and (b) sagittal plane.

The distribution of the shear strain E_{Shear} is given for the 7 subjects in Figs. 5 and 6 (respectively in the frontal and sagittal planes) below.

Except for subject 1 and 6, the shear strain was larger in the sagittal plane as compared to the frontal plane. On average, the shear strain was equivalent for subject 1 in both planes and larger in the frontal plane for subject 6. Results also show a high inter-individual variability in the mechanical response.

Table 1 below gives the average values of the strains in the first and second principal directions over the grid for each subject for both planes. For the first principal direction, it can be observed that strains in both planes are of the same intensity. It can also be observed that the strains in the first principal direction (compression) are lower than the strains in the second principal direction (tension in frontal and sagittal planes).

3.3. Intra operator reproducibility

The distribution of the error of reproducibility $\mathbf{S_i}$ of the shear strain is reported in Fig. 3 below in the form of a box-plot in the frontal and sagittal planes for each subject. The average error was below 2% in the frontal plane and 3% in the sagittal plane.

4. Discussion

The present work aimed to show the feasibility of using B-mode ultrasound imaging for the quantification of internal soft-tissue strains of buttock tissues in two perpendicular planes during sitting. A methodology was proposed for measuring subdermal soft tissue displacements and mapping strains in the frontal and sagittal planes respectively using DIC. Our results show that soft tissue in the fat layer can be tracked. On the contrary, the soft tissue displacement in the muscle region beneath the ischial tuberosity could not always be assessed due to the limited lateral field of view of the device. The method included a manual correction phase which was performed by the same operator for all the subjects. To ensure the reliability of the strain measurements, the repeatability of this operator was also quantified and shown to be inferior to 3% for the shear strain in the fat tissue in both the frontal and sagittal planes.

If the quantification of the soft tissue strain field has gained increasing interest in static, dynamic and transient elastography for the clinical diagnosis of various diseases in the last years, this is, as far as the authors are aware of, the first time that B-mode ultrasound imaging is used for the quantification of subdermal soft tissue strains in the buttock region. Previous studies focused on the ultrasound strain mapping of the human Achilles tendon [27], quadriceps muscle [28], carotid artery [29] and breast [30] for example. The assessment of the strains in the buttock region implies several specific difficulties due to the limited accessibility to the zone, the deep position of the osseous structures and the necessity to localize the ischial tuberosity. Other attempts have been made with MRI to assess the deformation of the tissue during sitting. Most of these studies did not report local strains [17,18]. Only Solis et al. used tagged MRI to quantify internal deformation in the buttocks of pigs [19]. However, this technic cannot be easily transposed in humans while sitting because of several limitations. First, the sequential acquisition of slices requires relatively large acquisition time at each load step, which prevents obtaining a continuous assessment over the sitting motion. Second, as the technic relies on the assumption of small deformations, the assessment of internal deformation during the sitting would necessitates a large number of loading step given the large deformation experienced by buttock soft

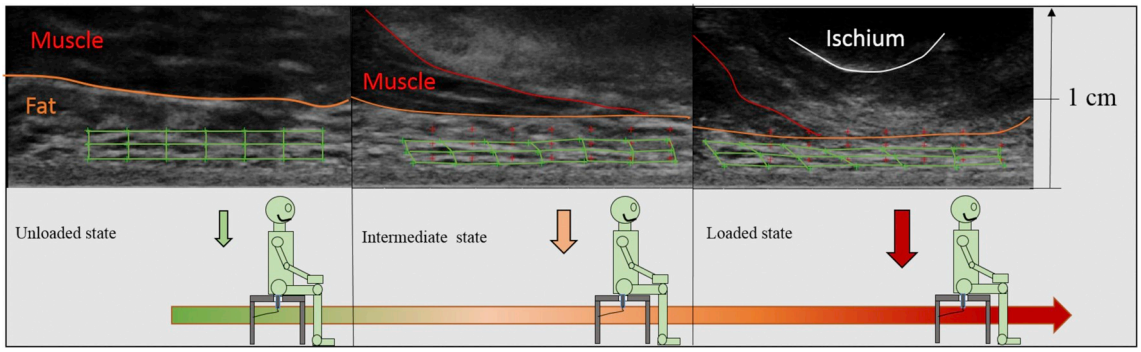

Fig. 4. Internal deformation of the subdermal soft tissues during sitting. The grid manually defined over the region of interest is superposed on the images.

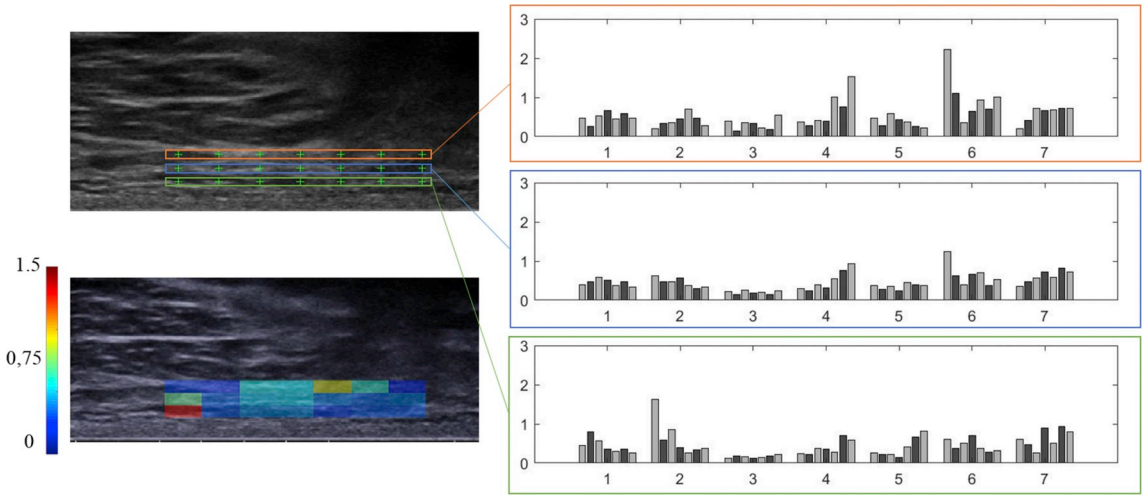

Fig. 5. Frontal plane. (a) initial grid superposed on the initial image (b) shear strain at each point of the grid for one typical subject (c) for each subject (abscissa 1 to 7 of the graph) a group of 7 bars gives the shear strain measured in each point of the grid.

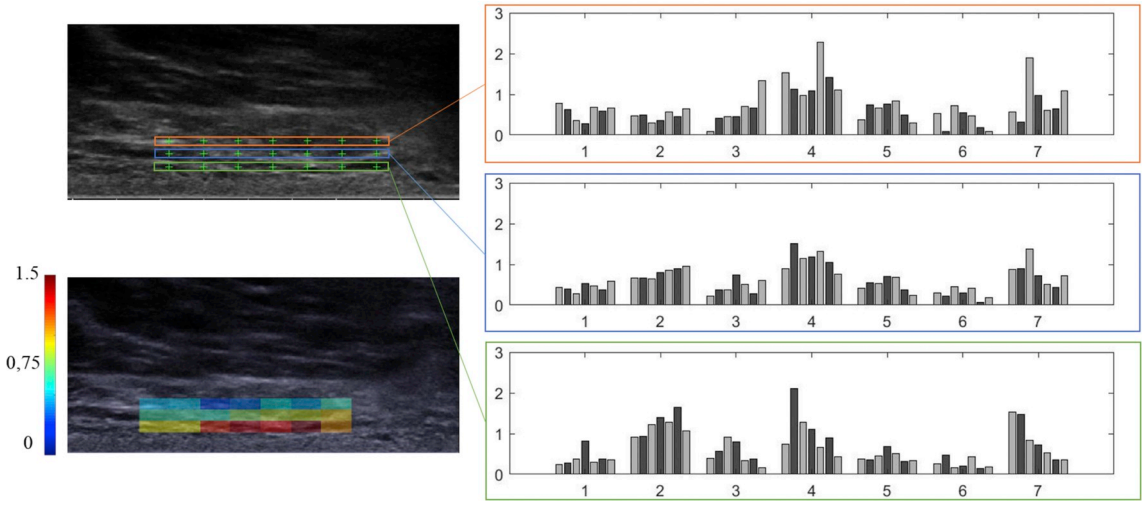

Fig. 6. Sagittal plane. (a) initial grid superposed on the initial image (b) shear strain at each point of the grid for one typical subject (c) for each subject (abscissa 1 to 7 of the graph) a group of 7 bars gives the shear strain measured in each point of the grid.

tissue during sitting. Third, the initial unloaded sitting position in the MRI can only be simulated [31]. On the contrary, the present work allowed to image subdermal soft tissue response during the full progressive loading of the buttock during sitting motion and, from these, to compute internal soft-tissue strains of buttock in two perpendicular planes in a population of 7 healthy subjects.

In the present contribution, the monitoring of the muscle tissue during the whole acquisition was not always possible due to the limited acquisition field inherent to the use of ultrasound probes. Moreover, in both the frontal and sagittal planes, the muscle tissue motion in the second principal direction (perpendicular to the pelvis motion) was important suggesting there was a non-negligible out-of-plane motion of the material particles. As a result, tracking muscle features using image registration techniques in each plane would introduce biases. Accordingly, computing muscle tissue strains of buttock was not reported. Yet, the analysis of the videos allowed to observe the complex

Table 1
Average and standard deviation of the principal strains in the frontal and sagittal planes respectively.

Fat Tissue	Subject 1		Subject 2		Subject 3		Subject 4		Subject 5		Subject 6		Subject 7	
E_I(%) (standard deviation)	-34 (2)	-41 (2)	-37 (2)	-42 (1)	-27 (1)	-33 (2)	-40 (2)	-44 (2)	-32 (2)	-35 (2)	-36 (4)	-26 (4)	-41 (3)	-42 (3)
E_{II}(%) (standard deviation)	57 (14)	53 (15)	82 (8)	160 (8)	18 (12)	62 (56)	64 (27)	190 (49)	45 (17)	75 (20)	64 (10)	40 (11)	77 (11)	123 (45)

Frontal plane Sagittal plane

behaviour of this tissue layer during the loading. In particular, it was observed that the gluteus maximus and hamstring muscles did not always remain underneath the IT, but instead, in certain subjects, slided out of plane, leaving the IT on the fat tissue. This observation is close to previous reported results. Sonenblum et al. observed that the gluteus maximus had a posterior and lateral displacement between simulated unloaded and loaded sittings in an MRI [17,32]. This contributes to the decrease of the thickness of soft tissue muscle under the ischial tuberosity. These results should be further investigated because, if confirmed, it could question the assumptions, commonly made by teams developing finite element model of the buttock that deep tissue injury initiates in the muscle underlying the bone. Because the localised tissue strain is obviously directly linked to the morphology of the bones future work focusing on the relationship between localised soft tissue strains and bone morphology and surface orientation is also useful for better understanding the determinants of the onset of PU.

The values of shear strains in the fat layer reported in the present contribution in two perpendicular planes can reach levels higher than the damage thresholds determined *in vitro* on rat models [33]. It must be noticed that these thresholds concern muscle tissues. However, in a case study, Sonenblum et al. observed that a patient with a history of pelvic pressure ulcer had no muscle loaded while sitting, the gluteus maximus resting entirely posterior and lateral to the ischium [17]. This suggest that pressure ulcers can develop in the fat tissue. Considering the level of strains quantified in our study, we could expect that the strain damage thresholds would be different for the fat than for the muscle. Further studies are necessary to evaluate these thresholds.

The proposed methodology also allowed to quantify the deformation in two orthogonal planes. The quantification of the rotation of the pelvis between the two acquisitions confirm that the deviation from the orthogonal assumption could be neglected. Although analysis of full 3D strain field is more appropriate to characterize soft tissue deformation, the proposed protocol is a good alternative easier to implement and process. The results obtained also underlined that the shear strain intensity is of comparable magnitude in both the frontal and sagittal planes, which disconfirmed the assumption of plane deformation, usually made in finite element simulations.

In addition to the improvement of the proposed methodology to address the biases discussed in this section, future work should also focus on the validation of the localised strain field. One promising avenue is the adaptation of the “truth cube” method proposed by Kerdok et al. [35] where a physical standard (cube of silicone rubber with a pattern of embedded Teflon spheres loaded in uniaxial compression) was developed to validate a FE model. This raises several issues related to the realistic representation of the complexity of the subdermal soft tissues *in silico* and which will have to be addressed.

To conclude, this study gives one of the first experimental evaluation of the internal deformation in the buttock region in humans during a real sitting motion. One of the future perspective to assess deformation in the muscle would be to combine this protocol with an acquisition of the load exerted on the buttock to be able to assess the deformation at intermediate strain ranges when muscles remain visible in the field of view of the ultrasound device.

Conflicts of interest

The authors certify that no conflict of interest is raised by this work.

Acknowledgments

This work was supported by the Fondation de l'Avenir (grant number AP-RM-2016-030), by la Fondation des Arts et Métiers and the Fond de dotation Clinatec. The authors are also grateful to the ParisTech BiomecAM chair program on subject-specific musculoskeletal modeling.

References

[1] Agence Nationale d’Accreditation et d’Evaluation en Sante. Prevention and treatment of pressure ulcers of adults and elderly persons. Soins Gerontol 2002(35):41–7.
[2] Van Nie-Visser NC, Schols JMGA, Meesterberends E, Lohrmann C, Meijers JMM, Halfens RJG. An International prevalence measurement of care problems: study protocol. J Adv Nurs 2013;69(9).
[3] Cogan AM, Blanchard J, Garber SL, Vigen CL, Carlson M, Clark FA. Systematic review of behavioral and educational interventions to prevent pressure ulcers in adults with spinal cord injury. Clin Rehabil 2016;31(7):871–80.
[4] Ceelen KK, et al. Validation of a numerical model of skeletal muscle compression with MR tagging: a contribution to pressure ulcer research. J Biomech Eng 2008;130(6):061015.
[5] a Ankrom M, et al. Pressure-related deep tissue injury under intact skin and the current pressure ulcer staging systems. Adv Skin Wound Care 2005;18(1):35–42.
[6] Bouten CV, Oomens CW, Baaijens FP, Bader DL. The etiology of pressure ulcers: skin deep or muscle bound? Arch Phys Med Rehabil 2003;84(4):616–9.
[7] Gefen A. The biomechanics of sitting-acquired pressure ulcers in patients with spinal cord injury or lesions. Int Wound J 2007;4(3):222–31.
[8] Garber SL, Rintala DH, Hart KA, Fuhrer MJ. Pressure ulcer risk in spinal cord injury: Predictors of ulcer status over 3 years. Arch Phys Med Rehabil 2000;81(4):465–71.
[9] Krause JS, Broderick L. Patterns of recurrent pressure ulcers after spinal cord injury: Identification of risk and protective factors 5 or more years after onset. Arch Phys Med Rehabil 2004;85(8):1257–64.
[10] Richardson RR, Meyer PR. Prevalence and incidence of pressure sores in acute spinal cord injuries. Paraplegia 1981;19(4):235–47.
[11] Brem H, Lyder C. Protocol for the successful treatment of pressure ulcers. Am J Surg 2004;188(1 SUPPL):1.
[12] Stekelenburg A, et al. Role of ischemia and deformation in the onset of compression-induced deep tissue injury: MRI-based studies in a rat model. J. Appl. Physiol. Bethesda Md 1985 2007;102(5):2002–11.
[13] Loerakker S, et al. The effects of deformation, ischemia, and reperfusion on the development of muscle damage during prolonged loading. J Appl Physiol Oct. 2011;111(4):1168–77.
[14] Ceelen KK, et al. Compression-induced damage and internal tissue strains are related. J Biomech 2008;41(16):3399–404.
[15] Gawlitta D, Li W, Oomens CWJ, Baaijens FPT, Bader DL, Bouten CVC. The relative contributions of compression and hypoxia to development of muscle tissue damage: an in vitro study. Ann Biomed Eng 2007;35(2):273–84.
[16] Gefen A, van Nierop B, Bader DL, Oomens CW. Strain-time cell-death threshold for skeletal muscle in a tissue-engineered model system for deep tissue injury. J Biomech 2008;41(9):2003–12.
[17] Sonenblum SE, Sprigle SH, Cathcart JMK, Winder RJ. 3D anatomy and deformation of the seated buttocks. J Tissue Viability 2015;24(2):51–61.
[18] Call E, Hetzel T, McLean C, Burton JN, Oberg C. Off loading wheelchair cushion provides best case reduction in tissue deformation as indicated by MRI. J Tissue Viability 2017;26(3):172–9.
[19] Solis LR, et al. Distribution of internal strains around bony prominences in pigs. Ann Biomed Eng 2012;40(8):1721–39.
[20] Luboz V, et al. “Personalized modeling for real-time pressure ulcer prevention in sitting posture. J Tissue Viability 2017:2–6.
[21] Linder-Ganz E, Shabshin N, Gefen A. Patient-specific modeling of deep tissue injury biomechanics in an unconscious patient who developed myonecrosis after prolonged lying. J Tissue Viability 2009;18(3):62–71.
[22] Al-Dirini RMA, Reed MP, Hu J, Thewlis D. Development and validation of a high Anatomical Fidelity FE model for the buttock and thigh of a seated individual. Ann Biomed Eng 2016;44(9):2805–16.
[23] Linder-ganz E, Shabshin N, Itzchak Y, Yizhar Z, Siev-ner I, Gefen A. Strains and stresses in sub-dermal tissues of the buttocks are greater in paraplegics than in healthy during sitting vol. 41. 2008. p. 567–80.
[24] Klauser AS, Miyamoto H, Bellmann-Weiler R, Feuchtner GM, Wick MC, Jaschke WR. Sonoelastography: musculoskeletal applications. Radiology 2014;272(3):622–33.
[25] Gennisson J-L, Deffieux T, Fink M, Tanter M. Ultrasound elastography: Principles and techniques. Diagn. Interv. Imaging May 2013;94(5):487–95.
[26] Haijiang Zhu JZ, Zhou Shifeng, Yang Ping, Longbiao He. An efficient optimal method for a 2D strain estimation of ultrasound tissue-mimicking material phantom. Polym Eng Sci 2015;55(12):2751–60.
[27] Chimenti RL, Flemister AS, Ketz J, Bucklin M, Buckley MR, Richards MS. Ultrasound strain mapping of Achilles tendon compressive strain patterns during dorsiflexion. J Biomech 2016;49(1):39–44.
[28] Affagard JS, Feissel P, Bensamoun SF. Measurement of the quadriceps muscle displacement and strain fields with ultrasound and Digital Image Correlation (DIC) techniques. Irbm 2015;36(3):170–7.
[29] Lee Gahyun, Jeon Sunghoon, Lee Sang-Kwon, Kim Hyunwoo, Yu Dohyeon, Choi Jihye. Strain elastography using dobutamine-induced carotid artery pulsation in canine thyroid gland. Vet Radiol Ultrasound Jul. 2015;56(5):549–53.
[30] Mutala TM, Ndaiga P, Aywak A. Comparison of qualitative and semiquantitative strain elastography in breast lesions for diagnostic accuracy. Canc Imag May 2016;16.
[31] Al-Dirini RMA, Reed MP, Thewlis D. Deformation of the gluteal soft tissues during sitting. Clin Biomech 2015;30(7):662–8.
[32] Sonenblum SE, Sprigle SH, Cathcart JMK, Winder RJ. 3-dimensional buttocks response to sitting: a case report. J Tissue Viability 2013;22(1):12–8.
[33] Loerakker S, et al. Temporal effects of mechanical loading on deformation-induced damage in skeletal muscle tissue. Ann Biomed Eng 2010;38(8):2577–87.
[34] Vergari C, Mansfield J, Meakin JR, Winlove PC. Lamellar and fibre bundle mechanics of the annulus fibrosus in bovine intervertebral disc. Acta Biomater 2016;37:14–20.
[35] Kerdok AE, Cotin SM, Ottensmeyer MP, Galea AM, Howe RD, Dawson SL. Truth cube: Establishing physical standards for soft tissue simulation. Med Image Anal 2003;7(3):283–91.